

Supporting Information

Effects of functional graft polymers on phase separation and ion-channel structures in anion exchange membranes analyzed by SANS partial scattering function

Kimio Yoshimura,¹ Akihiro Hiroki,¹ Aurel Radulescu,² Yohei Noda,³ Satoshi Koizumi,³

Yue Zhao,^{1,*} Yasunari Maekawa^{1,*}

¹Department of Advanced Functional Materials Research, Takasaki Institute for Advanced Quantum Science, National Institutes for Quantum Science and Technology (QST), Watanuki-machi 1233, Takasaki, Gunma, 370-1292, Japan

²Forschungszentrum Jülich GmbH, Jülich Centre for Neutron Science @ MLZ, Lichtenbergstraße 1, D-85747 Garching, Germany

³Department of Engineering, Ibaraki University, Hitachi 316-8511, Japan

S1. Preparation and characterization of radiation-grafted AEMs.

S1.1 AEM preparation and property characterization

ETFE films (Tefzel 100LZ, mass density (d_{ETFE}) = 1.7 g/cm³, crystallinity (X_c) = 0.36) with a thickness of 25 μm were purchased from DuPont and used as a base film. Iodomethane was purchased from Tokyo Chemical Industry Co., Ltd. St, ethanol, potassium hydroxide (KOH), hydrochloric acid (HCl), and 0.1 mol/l sodium hydroxide solution (NaOH) were purchased from Wako Pure Chemical Industries, Ltd. These chemicals were used without further purification. 1,4-Dioxane that was obtained from Wako Pure Chemical Industries, Ltd. as well was dried over molecular sieves before use. The water used in the experiments was purified using a Millipore Milli-Q UV system and had a resistance of 18.2 M Ω cm and a total organic carbon content of < 10 ppb.

ETFE films were put in a Schlenk tube and irradiated using a ⁶⁰Co γ -ray source (QST

Takasaki, Gunma, Japan) at room temperature in argon atmosphere with a total dose of 80 or 160 kGy at a dose rate of 10 kGy h⁻¹. Pre-irradiated ETFE films were immediately immersed in argon-purged monomer solutions (50 ml) consisting of a mixture of Im and St with volume ratios of 90:10 and 75:25 in 1,4-dioxane (50 wt%), before they were heated under argon atmosphere at 60 °C for 2 and 24 h, respectively. The total dose for the samples having Im:St volume ratios of 90:10 was 80 kGy and that for the one having Im:St volume ratios of 75:25 was 160 kGy. The grafted ETFE was taken out and then washed three times using 100 ml 1,4-dioxane at room temperature, followed by refluxing using 200 ml ethanol for 2 h to extract residual monomers and homopolymers. The obtained films were dried under vacuum at 80 °C for 4 h. The GD of an AEM was estimated using Eq. (S1)

$$GD(\%) = \frac{w_g - w_0}{w_0} \times 100\% \quad (S1)$$

where w_0 and w_g are the weights of membranes before and after grafting in the dry state, respectively.

For *N*-alkylation, the grafted films were immersed in a 1 M dioxane solution of iodomethane (120 ml) under argon atmosphere at 60 °C for 24 h. The films were washed several times using dioxane of 30 ml. The films were then immersed in 120 ml 1M HCl/dioxane solution (50/50 vol%) to replace iodide (I⁻) to chloride (Cl⁻). The solution was exchanged three times every hour to ensure the completion of the ion-exchange reaction. The films were removed from the solution and washed using deionized water. Finally, the films were dried in a vacuum oven at 80 °C for 24 h.

The molar ratio of Im to St units (Im/St) in a graft polymer was estimated from the molar numbers of Im and St in a certain membrane (m_{Im} and m_{St}) by gravimetric changes during *N*-alkylation, given that the *N*-alkylation proceeded quantitatively, as the following

equations.

$$Im/St = m_{Im}/m_{St}$$

$$m_{Im} = (W_{Cl} - W_g)/M_{MeCl}$$

$$m_{St} = \frac{W_g - W_{Im}}{M_{St}} = (W_g - m_{Im}M_{2MeNVIm})/M_{St} \quad (S2)$$

where W_{Cl} , W_g , and W_{Im} are weights of a dry AEM with a chloride form, the precursor grafted membrane, and Im unit in the graft polymers, respectively. M_{MeCl} , M_{St} , and M_{Im} are molecular weights of MeCl (50.49 g/mol), St (104.15 g/mol), and Im (108.14 g/mol), respectively. The AEMs in a chloride form were then soaked in a 1 M KOH aqueous solution (100 ml) at room temperature for 6 h or in a 1 M NaHCO₃ aqueous solution (100 ml) to replace chloride (Cl⁻) in the film to hydroxide (OH⁻) or bicarbonate (HCO₃⁻). The molecular structure of copolymers in the graft polymers was confirmed by ¹³C solid-state NMR spectrum as shown Ref. 12.

The ion-exchange capacity (IEC) of an AEM was determined using a standard back titration method. The membrane in OH⁻ form was immersed in 15 mL of 0.1 N HCl solution (V_{ref} , ml) for 24 h. The solution was then titrated with a standard NaOH (0.1 N) solution (V_{mem} , ml) to pH = 7.0 by an automatic titrator (HIRANUMA COM-555). Subsequently, the membranes were washed and immersed in deionized water for 24 h to remove the residual HCl and then dried under vacuum at 50 °C overnight and weighed to determine the dry masses in the Cl⁻ form. The experimental IEC value was calculated using the following equation: $IEC = C \times (V_{ref} - V_{mem})/W_{dry}$ where C is the concentration of NaOH solution and W_{dry} is the mass of dry AEMs.

The WU of an AEM was calculated by the weight measurements as

$$WU(\%) = \frac{W_{wet} - W_{dry}}{W_{dry}} \times 100\% \quad (S3)$$

where W_{wet} represents the weight of the AEM in the hydrated state. To measure WU, the AEM was completely hydrated in water and lightly wiped with Kimwipes to remove the excess water on the surface before weighing.

Note that in this study, WU of AEMs was estimated from H₂O-swollen membranes, where the mass density of water (d_w) is 1.0 g/cm³. Thus, the total water volume fraction (ϕ_w) of wet AEMs can be calculated as

$$\phi_w = \frac{\frac{WU/100(1+GD/100)}{d_w}}{\frac{1}{d_{ETFE}} + \frac{GD/100}{d_{graft}} + \frac{WU/100(1+GD/100)}{d_w}} \quad (\text{S4})$$

where d_{graft} is the mass density of the grafts, being ~ 0.98 and 1.03 g/cm³ for AEM_IS64 and AEM_IS37, respectively.¹² Similarly, the volume fractions of ETFE ($\phi_{ETFE} =$

$$\frac{\frac{1}{d_{ETFE}}}{\frac{1}{d_{ETFE}} + \frac{GD/100}{d_{graft}} + \frac{WU/100(1+GD/100)}{d_w}} \text{) and grafts } (\phi_{graft} = \frac{\frac{GD/100}{d_{graft}}}{\frac{1}{d_{ETFE}} + \frac{GD/100}{d_{graft}} + \frac{WU/100(1+GD/100)}{d_w}} \text{) were}$$

estimated as listed in Table 1 in the main text.

The anion conductivity of an AEM was measured in the plane direction at 100 kHz using four-point probe alternating current (AC) electrochemical impedance spectroscopy (EIS) with an electrode system connected to an LCR meter (HIOKI 3522 LCR HiTESTER) at a desired temperature. The AEM was fully hydrated in nitrogen-saturated deionized water and placed between two platinum electrodes. The anion conductivity σ (mS/cm) was calculated from the obtained resistance R (Ω) according to the following equation.

$$\sigma \text{ (mS/cm)} = L/(S \times R) \times 10^3 \quad (\text{S5})$$

where L (cm) is the distance between two electrodes and S (cm²) is the cross-sectional area of the membrane obtained by multiplying the membrane thickness with the membrane width.

S1.2 SANS characterization

CV-SANS measurements were performed on KWS-2 SANS diffractometer operated by Juelich Centre for Neutron Science at the neutron source Heinz Maier-Leibnitz (FRM II reactor) in Garching, Germany.³³ The incident neutron beam at KWS-2 was monochromatized with a velocity selector to have the average wavelength (λ) of 5 Å with a wavelength resolution of $\Delta\lambda/\lambda = 20\%$. AEMs were measured in their bicarbonate (HCO_3^-) form to prevent degradation that is often observed in their hydroxide form. Before the SANS experiments, hydrated AEMs were prepared by equilibrating the membranes in water mixture with prescribed $\text{H}_2\text{O}/\text{D}_2\text{O}$ ratio at room temperature for 24 h. Then hydrated membranes were placed in SANS sample cells sealed by two quartz-plate windows with a silicon spacer in between to prevent evaporation, and then put on the neutron beam. All SANS measurements for both dry and hydrated AEMs were performed at room temperature. The scattering patterns were collected using a two-dimensional (2D) scintillation detector and circularly averaged to obtain scattering intensity profiles as a function of q , where q is the scattering vector and defined as $q = (4\pi/\lambda)\sin(\theta/2)$, where θ is the scattering angle. The operable q -range in CV-SANS experiments is $0.03 < q < 5 \text{ nm}^{-1}$. To confirm the scattering spectra at high- q range, conventional SANS measurements on dry AEMs were performed on an IBARAKI materials design diffractometer (iMATERIA) at the Japan Proton Accelerator Research Complex (J-PARC) under a user program (proposal No. 2022B0040). The final intensity profiles obtained were corrected for the background of the cell, the electronic noise of the detector, detector sensitivity, and incoherent scattering.

S1.3 The kinetics of the radiation-induced graft polymerization on fluoropolymer substrates

The radiation-induced polymerization is generally governed by many factors such as irradiation condition, substrate polymer and monomer chemistry, grafting reaction condition.⁴⁷ Specific to our samples made by preirradiation method, there are two main factors greatly influence the reaction kinetics. One is the ability of the substrate polymer to trap and stabilize radiation-induced radicals in its structure, and the other one is the monomer diffusion to the substrate polymer.

The radical trapping ability is a crucial parameter for radiation-induced polymerization, notably in the preirradiation method. It has been reported that at a high dose, radicals are mainly trapped in the crystalline regions, almost no trapped radicals are observed in the amorphous phase for semicrystalline fluoropolymers.^{S1-S3} The monomer reactivity significantly depends on its diffusion to the substrate polymer where radicals exist. In the case of semi-crystalline fluoropolymers, which barely swell in monomer and solvent mixture, the monomer diffusion is limited in the amorphous phase rather than the crystalline phase.⁴⁷ Further work on polystyrene grafting onto fluoropolymers by field-emission scanning electron microscopy observation has shown that radicals are primarily located at the interface of crystallites-amorphous zones, and the grafted polystyrene network essentially localized on the spherulite lamellae.^{S4}

As a result, the graft polymerization kinetics in ETFE-based AEMs can be described by the swelling of the ETFE amorphous domains, the diffusion of monomer into the swollen domains, the reaction of monomer and radical at the interface of ETFE crystallites, and subsequent graft polymer chain propagation in amorphous ETFE domains.

S2. Incompressibility assumption for a ternary system

Assuming a ternary system with 3 different components, the scattering intensity

can be split into partial scattering functions according to the scattering theory as follows:^{S5,}

S6

$$I(q) = \sum_{i=1}^3 b_i^2 S_{ii}(q) + 2 \sum_{i<j}^3 S_{ij}(q) \quad (S6)$$

S_{ii} is PSF self-term, defined as

$$S_{ii}(q) = \frac{1}{V} \langle \iint \delta\varphi_i(\vec{r}) \delta\varphi_i(\vec{r}') \exp \left[-i\vec{q} \cdot (\vec{r} - \vec{r}') \right] d\vec{r} d\vec{r}' \rangle \quad (S7)$$

where V is the scattering volume and $\delta\varphi_i(\vec{r})$ is the fluctuation part of the volume fraction of the i component at position \vec{r} ($\varphi_i(\vec{r})$), which is expressed as

$$\delta\varphi_i(\vec{r}) = \varphi_i(\vec{r}) - \bar{\varphi}_i \quad (S8)$$

where $\bar{\varphi}_i$ is the average volume fraction of the i component (*i.e.*, $\bar{\varphi}_i = \frac{1}{V} \int \varphi_i(\vec{r}) d\vec{r}$).

The definition in Eq. (S7) indicates that $S_{ii}(q)$ is the Fourier transform of the correlation function $[\gamma_i(\vec{u})]$ of $\delta\varphi_i(\vec{r})$, given by

$$\gamma_i(\vec{u}) = \int \delta\varphi_i(\vec{r}) \delta\varphi_i(\vec{r} + \vec{u}) d\vec{r} \quad (S9)$$

As $\gamma_i(\vec{u})$ specifies how $\delta\varphi_i(\vec{r})$ and $\delta\varphi_i(\vec{r}')$ in neighboring regions separated by \vec{u} correlate with each other in the real space, $S_{ii}(q)$ gives the structural information of the i component.

$S_{ij}(q)$ ($i \neq j$) is the PSF cross-term, defined by the following equation

$$S_{ij}(q) = \frac{1}{V} \langle \iint \delta\varphi_i(\vec{r}) \delta\varphi_j(\vec{r}') \exp \left[-i\vec{q} \cdot (\vec{r} - \vec{r}') \right] d\vec{r} d\vec{r}' \rangle \quad (S10)$$

According to the incompressibility assumption, we have

$$\sum_{i=1}^3 \delta\varphi_i(\vec{r}) = 0 \quad (S11)$$

Multiplying Eq. (S10) by $\delta\varphi_k(\vec{r}') \exp \left[-i\vec{q} \cdot (\vec{r} - \vec{r}') \right]$ and doing the integration over the scattering volume, we obtain

$$\sum_{i=1}^3 S_{ki}(q) = 0 \quad (S12)$$

where $1 \leq k \leq 3$. Eq. (S12) leads to

$$S_{kk}(q) = -\sum_{i \neq k}^3 S_{ki}(q) = \sum_{i \neq k}^3 S_{ii}(q) + 2 \sum_{i,j \neq k, i < j}^3 S_{ij}(q) \quad (\text{S13})$$

From Eq. (S13), we have

$$2S_{12} = S_{33} - S_{11} - S_{22} \quad (\text{S14})$$

$$2S_{13} = S_{22} - S_{11} - S_{33} \quad (\text{S15})$$

$$2S_{23} = S_{11} - S_{22} - S_{33} \quad (\text{S16})$$

Eqs. (S14) to (S16) mean that all the cross-terms can be substituted by the self-terms.

Therefore, the scattering intensity can be described only by the self-terms, S_{ii} . Thus Eq.

(S6) can be rewritten to

$$I(q) = (b_1 - b_2)(b_1 - b_3)S_{11}(q) + (b_2 - b_1)(b_2 - b_3)S_{22}(q) + (b_3 - b_1)(b_3 - b_2)S_{33}(q) \quad (\text{S17})$$

Which is Eq. (1) in the main text. On the basis of the incompressibility assumption, the number of partial scattering functions to express $I(q)$ is reduced from 6 in Eq. (S6) to 3 in Eq. (S17).

S3. Decomposition of scattering intensity profiles into partial scattering functions by contrast variation SANS.

When the SANS experiments are performed on the same sample with m different contrast by using $\text{H}_2\text{O}/\text{D}_2\text{O}$ mixtures, the obtained $I(q)$ s (as shown in Figures S1(a) and S1(b) with symbols) in CV-SANS experiments represent a group of linear equations as expressed in Eq. (1) in the main text and below

$$\begin{pmatrix} I_1(q) \\ \vdots \\ I_m(q) \end{pmatrix} = \mathbf{M} \cdot \begin{pmatrix} S_{11}(q) \\ S_{22}(q) \\ S_{33}(q) \end{pmatrix} \quad (\text{S18})$$

with each individual $I_i(q)$ being a linear equation in the i th measurement, described by the three PSF self-terms as shown in Eq. (1) in the main text.

$$I_i(q) = (b_1 - b_2)(b_1 - b_3)S_{11}(q) + (b_2 - b_1)(b_2 - b_3)S_{22}(q) + (b_3 - b_1)(b_3 - b_2)S_{33}(q) \quad (\text{S19})$$

\mathbf{M} is the coefficient matrix of the difference in SLD, as expressed in Eq. (S20) below,

$$\mathbf{M} = \begin{pmatrix} {}^1\Delta_{12} & {}^1\Delta_{13} & {}^1\Delta_{21} & {}^1\Delta_{23} & {}^1\Delta_{31} & {}^1\Delta_{32} \\ \vdots & \vdots & \vdots & \vdots & \vdots & \vdots \\ {}^m\Delta_{12} & {}^m\Delta_{13} & {}^m\Delta_{21} & {}^m\Delta_{23} & {}^m\Delta_{31} & {}^m\Delta_{32} \end{pmatrix} \quad (\text{S20})$$

where ${}^m\Delta_{ij} = {}^m(b_i - b_j)$ is the SLD difference between i and j in m th measurement.

In order to obtain three PSF self-terms in the right side of Eq. (S18), mathematically the inverse matrix \mathbf{M}^{-1} for every three intensities profiles, *i.e.* $I_\alpha(q)$, $I_\beta(q)$ and $I_\gamma(q)$, can be found, then $S_{ii}(q)$ can be mathematically calculated as

$$\begin{pmatrix} S_{11}(q) \\ S_{22}(q) \\ S_{33}(q) \end{pmatrix} = \mathbf{M}^{-1} \cdot \begin{pmatrix} I_\alpha(q) \\ I_\beta(q) \\ I_\gamma(q) \end{pmatrix} \quad (\text{S21})$$

The best solution of $S_{ii}(q)$ is determined by evaluating the consistency between the reconstructed SANS $I(q)$ profiles and the experimental ones using Eq. (S18) via back-substitution. In this study, the best solution of $S_{ii}(q)$ for AEM_IS64 is shown below,

$$\begin{pmatrix} S_{BP-BP}(q) \\ S_{GP-GP}(q) \\ S_{W-W}(q) \end{pmatrix} = \begin{pmatrix} -5.80E(-21) & 9.08E(-22) & 9.52E(-21) \\ 2.38E(-21) & -1.92E(-22) & 2.44E(-21) \\ -2.69E(-21) & 9.13E(-22) & 1.78E(-21) \end{pmatrix} \cdot \begin{pmatrix} I_{D60}(q) \\ I_{D100}(q) \\ I_{D40}(q) \end{pmatrix} \quad (\text{S22})$$

The best solution of $S_{ii}(q)$ for AEM_IS37 is given as,

$$\begin{pmatrix} S_{BP-BP}(q) \\ S_{GP-GP}(q) \\ S_{W-W}(q) \end{pmatrix} = \begin{pmatrix} -9.40E(-21) & 1.82E(-21) & 1.28E(-20) \\ 1.1E(-21) & -1.37E(-22) & 4.21E(-21) \\ -3.09E(-21) & 1.14E(-21) & 1.94E(-21) \end{pmatrix} \cdot \begin{pmatrix} I_{D65}(q) \\ I_{D100}(q) \\ I_{D45}(q) \end{pmatrix} \quad (\text{S23})$$

where $I_{D60}(q)$, $I_{D100}(q)$ and $I_{D40}(q)$ in Eq. (S22) are experimental CV-SANS intensity profiles of AEM_IS64 at $f_{D2O} = 60\%$, 100% and 40% , respectively. $I_{D65}(q)$, $I_{D100}(q)$ and $I_{D45}(q)$ in Eq. (S23) are experimental CV-SANS intensity profiles of AEM_IS37 at $f_{D2O} = 65\%$, 100% and 45% , respectively.

Using $S_{ii}(q)$ given by Eqs. (S22) and (S23), the reconstructed $I(q)$ profiles (solid lines) are well matched to the experimental profiles (symbols), as shown in Figure S1(a) and S1(b) in this supporting information, respectively, indicating the correctness of $S_{ii}(q)$.

S4. Hard-Sphere fluid model analysis.

For spheres with a size distribution, Gaussian distribution function is applied to modify $P(q)$ as below

$$P(q) = \int_0^\infty v^2 \left\{ \frac{3}{(qr)^3} [\sin(qr) - qr \cos(qr)] \right\}^2 \times \frac{1}{(2\pi)^{1/2} \sigma_R} \exp \left[-\frac{(r-R_s)^2}{2\sigma_R^2} \right] dr \quad (\text{S24})$$

where σ_R is the standard deviation of R_s .

Given that Percus–Yevick approximation accounts for the inter-particle interference, $S(q)$ is expressed as a function of the volume fraction of spheres (ϕ_s) and R_s .

$$S(q) = \frac{1}{1 + 24\phi_s \left(\frac{F(A)}{A} \right)} \quad (\text{S25})$$

where $A = 2qR_s$, ϕ_s is the volume fraction of spheres in the conducting domains, and $F(A)$ is a trigonometric function of A by

$$F(A) = \frac{\alpha}{A^2} (\sin A - A \cos A) + \frac{\beta}{A^3} (2A \sin A + (2 - A^2) \cos A - 2) + \frac{\gamma}{A^5} (-A^4 \cos A + 4[(3A^2 - 6) \cos A + (A^3 - 6A) \sin A + 6]) \quad (\text{S26})$$

where

$$\begin{aligned} \alpha &= (1 + 2\phi_s)^2 / (1 - \phi_s)^4 \\ \beta &= -6\phi_s \left(1 + \frac{\phi_s}{2} \right)^2 / (1 - \phi_s)^4 \\ \gamma &= \frac{1}{2\phi_s} (1 + 2\phi_s)^2 / (1 - \phi_s)^4 \end{aligned} \quad (\text{S27})$$

References:

- S1) Goslar, J.; Hilczner, B.; Smogór, H. Radiation-induced modification of P(VDF/TrFE) copolymers studied by ESR and vibrational spectroscopy. *Appl. Magn. Reson.* **2008**, *34*, 37–45.
- S2) Oshima, A.; Horiuchi, H.; Nakamura, A.; Kobayashi, S.; Terui, A.; Mino, A.; Shimura, R.; Washio, M. Trapped radical behavior of electron beam irradiated polytetrafluoroethylene fine powder at various temperatures, *Scientific Reports* **2021**, *11*, 10907.
- S3) Oshima, A.; Seguchi, T.; Tabata, Y. ESR study on free radicals trapped in crosslinked polytetrafluoroethylene(PTFE)-II radical formation and reactivity, *Radiat. Phys. Chem.* **1999**, *55*, 61-71.
- S4) Aymes-Chodur, C.; Betz, N.; Porte-Durrieu, M. -C.; Baquey, C.; Moel, A. L. A FTIR and SM study of PS radiation grafted fluoropolymers: influence of the nature of the ionizing radiation on the film structure, *Nucl. Instr. and Meth. in Phys. Res. B* **1999**, *151*, 377-385.
- S5) G. E. Bacon, *Neutron Diffraction*, Clarendon, Oxford, 1975.
- S6) J. S. Higgins and H. C. Benoit, *Polymers and Neutron Scattering*, Clarendon, Oxford, 1994.

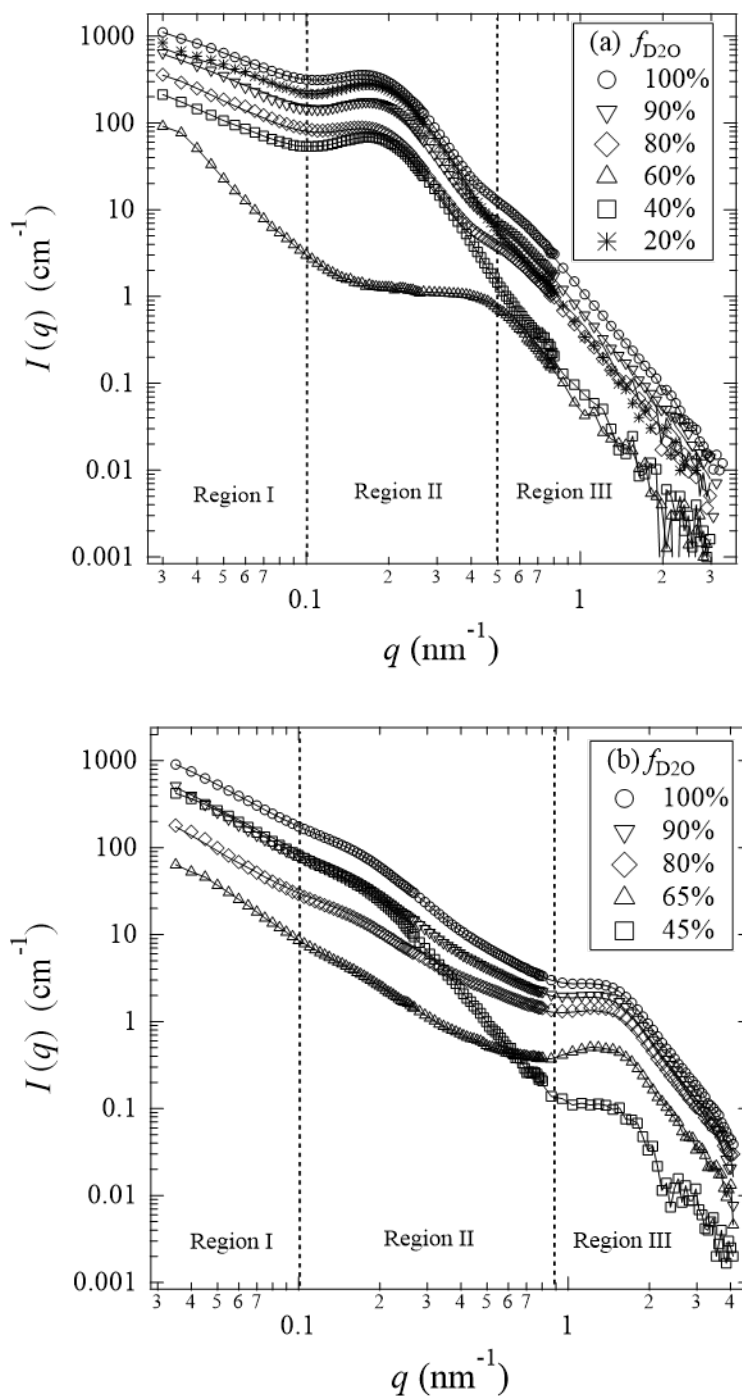


Figure S1 Experimental scattering intensity profiles (symbols) and the reconstructed intensity profiles (solid lines) of the hydrated (a) AEM_IS64; and (b) AEM_IS37, equilibrated in water mixtures of D₂O and H₂O with different ratios. (Adapted from Soft Matter 2018, 14, 9118-9131. Copyright [2018] Royal Society of Chemistry.)

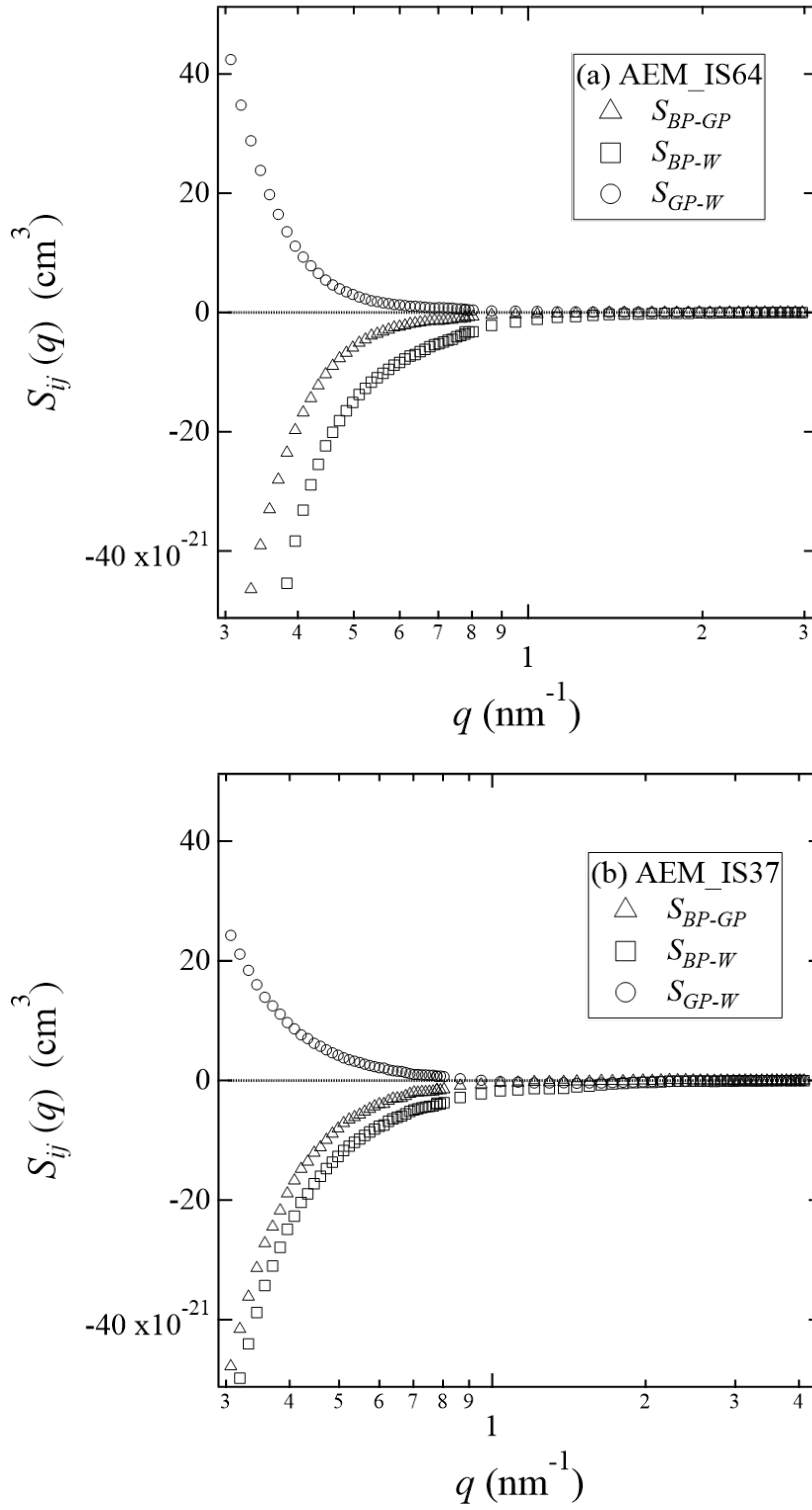


Figure S2 Enlarged PSF cross-terms of the hydrated (a) AEM_IS64, and (b) AEM_IS37.